NATIONAL ADVISORY COMMITTEE FOR AERONAUTICS

TECHNICAL NOTE 3554

A PRELIMINARY INVESTIGATION OF THE EFFECTS OF FREQUENCY AND AMPLITUDE ON THE ROLLING DERIVATIVES OF AN UNSWEPT-WING MODEL OSCILLATING IN ROLL

By Lewis R. Fisher, Jacob H. Lichtenstein, and Katherine D. Williams

Langley Aeronautical Laboratory
Langley Field, Va.

Washington
January 1956

NATIONAL ADVISORY COMMITTEE FOR AERONAUTICS

TECHNICAL NOTE 3554

A PRELIMINARY INVESTIGATION OF THE EFFECTS OF FREQUENCY AND AMPLITUDE ON THE ROLLING DERIVATIVES OF AN UNSWEPT-WING MODEL OSCILLATING IN ROLL

By Lewis R. Fisher, Jacob H. Lichtenstein,
and Katherine D. Williams

SUMMARY

A model with separable wing and tail assembly was oscillated in roll through a range of frequencies and amplitudes of oscillation for an angle of attack of 0° and at one frequency and amplitude for two higher angles of attack in order to determine the effects of the unsteady motion on the rolling stability derivatives of the model and its components.

A variation of frequency or amplitude of oscillation in the range covered at an angle of attack of 0° had no important effect on either the yawing moment due to rolling or the damping in roll for this unswept-wing airplane configuration. The only appreciable value of yawing moment due to rolling was shown by the fuselage-tail combination. This configuration experienced a reduction in magnitude of the derivative as either the frequency or the amplitude of the oscillation increased.

The values of the rolling derivatives obtained by oscillation were consistent with the values measured by means of conventional rolling-flow tests at an angle of attack of 0°. For the model with the wing at a high angle of attack, the oscillatory yawing moment due to rolling was different from that obtained under steady-state conditions.

INTRODUCTION

As part of a continuing investigation of the effects of unsteady motion on the lateral stability derivatives of airplane models, tests were made in the Langley stability tunnel at low speeds to determine the effects of frequency and amplitude on the yawing moment due to rolling and the damping in roll for an unswept-wing airplane model. These tests, which were preliminary in nature, involved the forced oscillation in roll of the model about its longitudinal wind axis through a range of

frequencies and amplitudes of motion. The results obtained were primarily for an angle of attack of 0°; however, some results for higher angles of attack are presented. Steady-state derivatives were measured by means of tests made with the model stationary in rolling flow and with the model rolling steadily at several rotary velocities in straight flow. These steady results are regarded as zero-frequency oscillation data and form the basis for a comparison of the unsteady-state and the steady-state rolling derivatives. Theoretical values for the steady-state rolling derivatives were also used for comparison with the experimental data.

The model used in these tests had a wing of aspect ratio 6 and a tail assembly, either of which could be separated from the fuselage. Tests were conducted for the fuselage alone, for the wing-off configuration, for the tail-off configuration, and for the complete model. The contribution of the vertical tail to the damping in yaw of a model of similar configuration measured during free oscillation in yaw is reported in reference 1 and during forced oscillation in yaw in reference 2.

SYMBOLS

The data are referred to the stability system of axes and are presented in the form of coefficients of the forces and moments about a point which corresponds to the normal location of the quarter-chord point of the wing mean aerodynamic chord of the model tested. (See fig. 1.) The coefficients and symbols used herein are defined as follows:

A aspect ratio, $\frac{b^2}{S}$

b wing span, ft

C_D drag coefficient, $\frac{\text{Drag}}{qS}$

C_L lift coefficient, $\frac{\text{Lift}}{qS}$

C_l rolling-moment coefficient, $\frac{L}{qSb}$

$$C_{l_p} = \frac{\partial C_l}{\partial\left(\frac{pb}{2V}\right)}$$

C_m pitching-moment coefficient, $\frac{M}{qS\bar{c}}$

C_n yawing-moment coefficient, $\frac{N}{qSb}$

$C_{n_p} = \frac{\partial C_n}{\partial\left(\frac{pb}{2V}\right)}$

ΔC_{n_p} vertical-tail increment to C_{n_p}, C_{n_p} (for fuselage + tail) - C_{n_p} (for fuselage)

C_Y lateral-force coefficient, $\frac{Y}{qS}$

$C_{Y_p} = \frac{\partial C_Y}{\partial\left(\frac{pb}{2V}\right)}$

c chord, ft

$\bar{c}$ mean aerodynamic chord, ft

f frequency, cps

I_X rolling moment of inertia, slug-ft^2

I_{XZ} product of inertia, slug-ft^2

L rolling moment, ft-lb

$L_{\dot{\phi}} = \frac{\partial L}{\partial \dot{\phi}}$

$L_{\ddot{\phi}} = \frac{\partial L}{\partial \ddot{\phi}}$

M pitching moment, ft-lb

N yawing moment, ft-lb

$N_{\dot{\phi}} = \frac{\partial N}{\partial \dot{\phi}}$

$N_{\ddot{\phi}} = \frac{\partial N}{\partial \ddot{\phi}}$

$p = \dot{\phi}$

q dynamic pressure, $\frac{1}{2}\rho V^2$, lb/sq ft

S wing area, sq ft

t time, sec

V free-stream velocity, ft/sec

Y lateral force, lb

X,Y,Z system of stability axes, (fig. 1)

α angle of attack, deg

λ taper ratio

ρ mass density of air, slugs/cu ft

ϕ angle of roll, deg or radians

$\dot{\phi} = \frac{\partial \phi}{\partial t}$

$\ddot{\phi} = \frac{\partial^2 \phi}{\partial t^2}$

$\omega = 2\pi f$

Subscripts:

w wing

t vertical tail

o amplitude

APPARATUS

Model

In order that the inertia in roll be kept as low as possible, the model, shown in figure 2, was constructed of spruce-reinforced balsa wood. The inertia of the complete model about its longitudinal axis was 0.011 slug-ft^2. The wing of the model was essentially unswept, had an aspect ratio of 6, a taper ratio of 0.5, and was constructed with an NACA 65-110 (a = 1.0) airfoil section. The model components were made separable to allow testing of each of four configurations - a fuselage alone, a fuselage and wing, a fuselage and tail assembly, and the complete model. The tail assembly included both vertical and horizontal tails, shown in figure 2, which were not separable. A photograph of the model in the test section is shown as figure 3.

Model Support System

For the oscillation tests and a portion of the steady-state tests, the model was mounted on a two-component strain-gage balance at the quarter-chord point of the wing mean aerodynamic chord. The balance was attached to the end of the curved model-support sting shown in figure 3. As the angle of attack of the model changed, the strain-gage balance remained fixed with respect to the longitudinal wind axis so that the moments were measured with respect to the stability (or, for these tests, the wind) system of axes.

The model-support sting rotated in two bearing housings supported by a rigid V-shaped strut mounted on the tunnel wall inside the test section (fig. 4(a)). For the steady-state rolling-flow tests, the model was mounted on a single-strut support attached to a mechanical six-component balance system.

Oscillation Apparatus

The model was oscillated for a range of amplitudes and frequencies by the equipment shown in the photographs of figure 4. A motor-generator set supplied direct current for a one-horsepower motor which turned a flywheel through suitable reduction gearing. The motor and flywheel were mounted on the tunnel wall outside the 6-foot-diameter circular test section of the Langley stability tunnel as shown in figure 4(b).

Sinusoidal motion was generated by means of a crank attached eccentrically to the flywheel and was transmitted to the model support sting through a push rod. A slide-wire roll-position indicator was mounted

on the upstream bearing housing of the model support strut with the rotating element fixed on the shaft of the model support sting. The position indicator was covered by the fairing shown in figure 5; this photograph shows a typical motion of the model during oscillation. The amplitude of the rolling motion was varied by adjusting the eccentricity of the crank at the flywheel. The frequency of oscillation was varied by a speed control that regulated the voltage to the driving motor.

For those tests in which the model was forced to roll steadily, the crank mechanism was replaced by a V-belt and pulley system with one pulley at the center of the flywheel and the other at the model support. (See fig. 6.) During these tests, it was necessary to balance the system about its axis of rotation by means of the counterweight shown in figure 6.

In order to eliminate the use of slip rings in the steady-rolling tests of the model, the strain-gage wires (fig. 6) were extended downstream about 50 feet where they were tied to a length of shock chord before being led outside the test section. The remaining end of the shock chord was tied to a downstream tunnel support. As the sting revolved and the strain-gage wires twisted, the shock chord stretched to keep the tension in the wires small. The wires were disconnected from the sting and uncoiled before the subsequent test run.

The entire oscillation apparatus was constructed and supported so as to be rigid and built to close tolerances in order to minimize lost motion and low-frequency vibrations which could be transmitted to the recording apparatus.

Recording of Data

During a test run at a constant amplitude and frequency of oscillation, a continuous and simultaneous oscillograph record was made of the yawing moment and the rolling moment, measured by the strain-gage balance, and of the displacement in roll of the model, measured by the roll-position indicator. The oscillograph also supplied a continuous time record. Some typical traces are shown in figure 7.

For those steady-state tests during which the model was sting-supported, the data were recorded in the same manner. When the model was strut-supported, forces and moments were recorded by the mechanical balance.

TESTS

Test Methods

This investigation involved the oscillation of a model in roll in order to determine the unsteady derivatives C_{n_p} and C_{l_p} for the complete model and its component parts. Variables for these oscillation tests included angle of attack, frequency of oscillation, and the amplitude of the rolling motion. As a basis for comparison with the unsteady derivatives, C_{n_p} and C_{l_p} were also measured under steady-state conditions. One series of these steady-state tests consisted of rolling the model at constant angular velocity in a straight airstream; the other steady-state tests involved rolling the air flow past the stationary model. In the latter method, moments were measured both by the strain-gage balance while the model was supported as in the oscillation tests and by a mechanical six-component wind-tunnel balance while the model was mounted on a single-strut support. The second of these is the standard procedure employed in the Langley stability tunnel for measuring the rolling-stability derivatives of models and is described in reference 3.

Test Conditions

All tests were conducted at a dynamic pressure of 24.9 pounds per square foot which corresponds to a free-stream velocity of 145 feet per second (under standard conditions), a Reynolds number of 442,000 based on the wing mean aerodynamic chord, and a Mach number of 0.13. The model was tested at angles of attack of 0°, 4°, and 8° by both the oscillation and the steady-state test procedures; however, because the reduction of the oscillograph data proved to be an extremely laborious process, it was deemed advisable to restrict the scope of the investigation to the following representative cases:

α, deg	f, cps	ϕ_o, deg
0	0.5 to 4.0	±5
0	1	±5 to ±20
0, 4, and 8	1	±5

The frequencies of the oscillation tests were chosen so that the range of the reduced-frequency parameter $\frac{\omega b}{2V}$ encompassed the range commonly encountered in the lateral oscillations of airplanes. This

parameter varied from $\frac{\omega b}{2V} = 0.030$ to $\frac{\omega b}{2V} = 0.243$. The actual frequencies of oscillation were 0.5, 1.0, 1.5, 2.0, 3.0, and 4.0 cycles per second. The large amplitudes of oscillation were chosen purposely to insure that the yawing moment would be of measurable magnitude. These amplitudes were ±5°, ±10°, ±15°, and ±20°.

For the tests in which the model was rolled at constant velocity, the circular velocities were 0, ±0.50, ±0.75, and ±1.00 revolutions per second which correspond to values of $\frac{pb}{2V}$ of 0, ±0.030, ±0.046, and ±0.061.

For those tests in which the model was stationary while the airstream was imparted a rolling velocity, the values of $\frac{pb}{2V}$ were 0.057, 0.029, 0.008, 0, -0.025, -0.043, and -0.065 in the case of the sting-mounted model and 0, ±0.023, ±0.046, and ±0.063 in the case of the strut-mounted model.

The following model configurations were tested: fuselage, wing, and tail (designated FWT), fuselage and wing (designated FW), fuselage and tail (designated FT), and fuselage (designated F).

REDUCTION OF DATA

The equations of equilibrium of rolling and yawing moments for a model mounted on a strain-gage balance and having a motion about its roll axis are

$$N = \left(N_{\ddot{\phi}} + I_{XZ}\right)\ddot{\phi} + N_{\dot{\phi}}\dot{\phi}$$

and

$$L = \left(L_{\ddot{\phi}} - I_X\right)\ddot{\phi} + L_{\dot{\phi}}\dot{\phi}$$

where L and N are the moments measured by the strain-gage balance. Since for this harmonic motion

$$\phi = \phi_o \cos 2\pi ft$$

and

$$\dot{\phi} = -\phi_o 2\pi f \sin 2\pi ft$$

then, at the time when $\phi = 0$,

$$\dot{\phi} = -\phi_o 2\pi f$$
$$\ddot{\phi} = 0$$

Therefore

$$(N)_{\phi=0} = N_{\dot{\phi}}\dot{\phi}$$

and

$$C_{n_p} = \frac{(N)_{\phi=0}}{qSb\frac{\dot{\phi}b}{2V}}$$

or

$$C_{n_p} = -\frac{2}{\pi\rho VSb^2}\frac{(N)_{\phi=0}}{\phi_o f}$$

Similarly, for the damping in roll,

$$C_{l_p} = -\frac{2}{\pi\rho VSb^2}\frac{(L)_{\phi=0}}{\phi_o f}$$

The terms $(N)_{\phi=0}$ and $(L)_{\phi=0}$ are, respectively, the yawing moment and the rolling moment measured when $\phi = 0$. These moments were read from the recorded oscillation data for each of five cycles of oscillation for each frequency and amplitude condition. The average reading was then used to compute the derivatives C_{n_p} and C_{l_p} from the expressions given above.

For the steady-state rolling results, the moment data were plotted against $\frac{pb}{2V}$. The slopes of C_n and C_l with respect to $\frac{pb}{2V}$ yielded the experimental values of C_{n_p} and C_{l_p}.

RESULTS AND DISCUSSION

Presentation of Results

The lift, drag, and pitching-moment data for the model and its component parts as determined for the investigation of reference 1 are reproduced in figure 8. The oscillatory derivatives C_{n_p} and C_{l_p}

are shown in figures 9 and 10, respectively, together with the steady-state derivatives obtained with the sting-mounted model in rolling-flow tests. The steady-state derivatives are presented for reference as zero-frequency values in figures 9(a) and 10(a), and as zero-amplitude values in figures 9(b) and 10(b). The latter is a matter of convenience because, strictly speaking, steady-state rolling does not, of course, correspond to a zero-amplitude motion.

Figure 11 represents the variation with frequency and amplitude of the vertical-tail contribution to C_{n_p} at $\alpha = 0^\circ$, obtained from the data of figure 9, both in the presence and in the absence of the wing. An indication of the probable error of the mean values of some of the oscillation data from which figure 9 was prepared is given in figure 12.

The rolling derivatives measured by three techniques are compared in figure 13. These methods include oscillation at constant frequency and amplitude, rolling the air flow with constant angular velocity (conventional rolling-flow technique), and rolling the model with constant angular velocity. The two latter methods, of course, yield steady-state results. The rolling-flow results in figure 13 include those for the model mounted on the sting support used for the oscillation tests as well as those for the model mounted on the conventional support strut.

Discussion

Yawing moment due to rolling.- For the model configurations other than the fuselage and tail, C_{n_p} is small, generally negative, and shows no consistent effect of frequency or amplitude at an angle of attack of 0° (fig. 9). The values of C_{n_p} for the fuselage and tail, which are the only values of any appreciable magnitude, in general tend to become somewhat smaller as either the frequency or amplitude increases. The fact that these changes in C_{n_p} with either frequency or amplitude are of the same order of magnitude might be expected because the magnitude of the rolling velocity p_o is the same for corresponding points along the curves of figures 9(a) and 9(b). It was shown in the section entitled "Reduction of Data" that the maximum rolling velocity depends on the product $\phi_o f$. Figures 9(a) and 9(b) are, then, the variations of C_{n_p} with the magnitude of rolling velocity as well as with the factors of amplitude and frequency of oscillation which determine the rolling velocity. These figures indicate that the effectiveness of the vertical tail of the fuselage-tail combination in producing C_{n_p} decreases somewhat as its angle of attack due to rolling $\frac{p_o b}{2V}$ is increased.

The largest value of C_{n_p} shown in figure 9 was contributed by the vertical tail of the fuselage-tail combination. The addition of the wing, however, reduced this vertical-tail contribution to a small value. This wing-interference effect has also been observed in previous rolling-flow experiments. The fact that this reduction in C_{n_p} is caused by wing interference rather than by the C_{n_p} contribution of the wing itself is seen by comparing the data for the fuselage alone and for the fuselage-wing configuration; the wing itself contributes only a small negative value to C_{n_p}. In the presence of the wing, however, the loading on the vertical tail due to rolling is effectively overcome by an opposite loading due to sidewash from the rolling wing as discussed in reference 4.

In order of magnitude, values of C_{n_p} obtained from oscillation tests agree very well, with one exception, with the steady-state values obtained in rolling flow at an angle of attack of 0°. The exception occurred for the complete model for which a small positive C_{n_p} was measured in rolling flow whereas the oscillatory values were also small but negative (fig. 9(a)). These rolling-flow results were for the model supported on the oscillation sting in the same manner as it was for the oscillation tests.

Increasing the angle of attack of the model from 0° to 8° at 1 cycle per second reduced the large value of C_{n_p} for the fuselage and tail by about 70 percent (fig. 9(c)). No particular effect of angle of attack was shown, however, on the rather small values of C_{n_p} exhibited by the other configurations.

The increments in C_{n_p} contributed by the tail both in the presence and in the absence of the wing are shown in figure 11 together with steady-state values calculated for the tail. The tail-alone value of C_{n_p} was calculated from the data of reference 5. This value is expected to be somewhat large for a tail surface because the loadings given in reference 5 are for one semispan of a complete rolling wing and contain some load carried over from the other semispan. The presence of the wing was taken into consideration by using the method presented in reference 4 to estimate the sidewash at the tail due to the wing load. The estimated reduction in the tail contribution to C_{n_p} due to the presence of the wing is in good agreement with the experimental results. Also shown clearly, in figure 11, is the overall reduction to the tail C_{n_p} resulting from an increase in either frequency or amplitude of oscillation.

Damping in roll.- The results shown in figure 10 indicate that at an angle of attack of 0° there are no important effects of unsteady motion on the damping in roll for the unswept-wing model tested. The values of C_{l_p} obtained by oscillation are consistent with those obtained by rolling flow with the model supported on the oscillation sting. The wing itself produced the largest increment of C_{l_p}. The presence of the wing reduced the contribution of the tail to C_{l_p} as it did for C_{n_p}, but this effect is insignificant because of the comparative smallness of the tail contribution to C_{l_p}.

An estimate of the steady-state contribution of the vertical tail to C_{l_p} may be made by methods similar to those for the C_{n_p} contribution. Such a calculation predicts a value of $\Delta C_{l_p} = -0.044$ for the tail in the absence of the wing and a value of $\Delta C_{l_p} = -0.027$ for the tail in the presence of the wing. These values are in agreement with the increments which can be obtained from figure 10.

An increase in angle of attack from 0° to 8° reduced the damping in roll of the wing by a considerable amount (fig. 10(c)). This reduction in C_{l_p} is roughly proportional to the change in the wing lift-curve slope between these angles. (See fig. 8.)

On the quality of the oscillation data.- In order to record the small yawing moments due to rolling, it was necessary that the sensitivity of the strain-gage yawing-moment beam be comparatively high. This high sensitivity resulted in a natural frequency in yaw of the order of 20 cycles per second for the strain gage with model attached. Because the model was excited by wind-tunnel turbulence or by unsteady vortex flow off the model, the oscillograph records show a trace with a frequency of 20 cycles per second due to these disturbances superimposed on the lower frequency trace due to the forced oscillation. (See fig. 7.) At an angle of attack of 0°, the superimposed noise had an amplitude comparable in magnitude to the amplitude of the oscillatory moment and it was very regular over a long period of time. It was not difficult, therefore, because of this regularity, to eliminate the high-frequency noise by fairing the trace as shown in figure 7.

In figure 12, the probable error of the arithmetic mean of the test points is shown for two of the model configurations that are presented in figure 9. This error represents the uncertainty in the average test values of C_{n_p} which results from the fairing procedure followed. Since a large number of data points for each frequency and amplitude

condition were averaged, the resulting data presented in figure 9 are believed to be fairly reliable.

As the angle of attack of the model was increased to 8°, the amplitudes of the high-frequency noise grew larger and had less uniformity than at $\alpha = 0°$ and 4°. These effects made the fairing of the yawing-moment trace somewhat more uncertain and probably reduce to some extent the reliability of the high-angle-of-attack data. At $\alpha = 8°$, the wing was partially stalled and there appeared to be considerable buffeting of the model.

For the rolling-moment trace, these problems were of less concern. The sensitivity of the strain gage in roll was only 10 percent of its sensitivity in yaw; as a result, the superimposed noise was of much higher frequency and of much smaller amplitudes than that for the corresponding yawing-moment trace as shown in figure 7. Although the noise again assumed greater amplitudes and less uniformity at $\alpha = 8°$, in general, the oscillatory values of C_{l_p} are considered to be reliable for all angles of attack.

Comparison of results obtained by different techniques.- A comparison of the oscillatory derivatives (for $f = 1$ cps and $\phi_o = \pm 5°$) with the steady-state derivatives measured by two methods (rolling flow and rolling model) is shown in figure 13. In general, these two steady-state techniques give approximately the same values of C_{n_p} and C_{l_p} at $\alpha = 0°$, with the exception of a difference in C_{n_p} for the models with the wing. This difference may be due in part to differences in support-strut interference. Although the previous discussion has shown that, for $\alpha = 0°$, frequency effects were small, the difference in C_{n_p} at $\alpha = 8°$ between the steady-state and the oscillation results may indicate large effects of frequency at the high angles of attack. A previous investigation (ref. 6) has shown that, for wings for which partial separation has occurred during unsteady motion, an aerodynamic lag may exist which contributes to the moments acting on the wing. Such an aerodynamic lag may cause the rolling-stability derivatives either of the wing itself or of the tail or fuselage in the presence of the wing to be markedly different from the steady-state derivatives at high angles of attack.

CONCLUSIONS

An unswept-wing model, which was tested as a fuselage alone, a fuselage-tail combination, a fuselage-wing combination, and a complete configuration, was oscillated in roll through a range of frequencies and amplitudes of oscillation to determine the effects of unsteady motion on the rolling-stability derivatives of the model and its components chiefly at an angle of attack of 0°. The results of this investigation indicate the following conclusions:

1. The only model configuration which exhibited yawing moment due to rolling of any appreciable magnitude was the fuselage-tail combination. For this configuration, an increase in either frequency or amplitude at an angle of attack of 0° resulted in a small reduction in the magnitude of the derivative; for the other configurations tested, yawing moment due to rolling was small and showed no important effect of frequency or amplitude. The large yawing moment due to rolling of the fuselage-tail combination was reduced to a small value in the presence of the wing. This wing-interference effect on the tail contribution to the derivative can be accurately estimated by means of existing steady-state theory.

2. Frequency or amplitude had no noticeable effect on the magnitude of the damping in roll for the model or any of its components at an angle of attack of 0°.

3. The rolling derivatives of the model and its components measured by the oscillation tests were generally consistent at low angles of attack with the derivatives measured by steady-state tests. At a high angle of attack the oscillatory yawing moment due to rolling for the model with the wing was different from that obtained under steady-state conditions.

Langley Aeronautical Laboratory,
National Advisory Committee for Aeronautics,
Langley Field, Va., October 19, 1955.

REFERENCES

1. Bird, John D., Fisher, Lewis R., and Hubbard, Sadie M.: Some Effects of Frequency on the Contribution of a Vertical Tail to the Free Aerodynamic Damping of a Model Oscillating in Yaw. NACA Rep. 1130, 1953. (Supersedes NACA TN 2657.)

2. Fisher, Lewis R., and Wolhart, Walter D.: Some Effects of Amplitude and Frequency on the Aerodynamic Damping of a Model Oscillating Continuously in Yaw. NACA TN 2766, 1952.

3. MacLachlan, Robert, and Letko, William: Correlation of Two Experimental Methods of Determining the Rolling Characteristics of Unswept Wings. NACA TN 1309, 1947.

4. Michael, William H., Jr.: Analysis of the Effects of Wing Interference on the Tail Contributions to the Rolling Derivatives. NACA Rep. 1086, 1952. (Supersedes NACA TN 2332.)

5. Bird, John D.: Some Theoretical Low-Speed Span Loading Characteristics of Swept Wings in Roll and Sideslip. NACA Rep. 969, 1950. (Supersedes NACA TN 1839.)

6. Fisher, Lewis R., and Fletcher, Herman S.: Effect of Lag of Sidewash on the Vertical-Tail Contribution to Oscillatory Damping in Yaw of Airplane Models. NACA TN 3356, 1955.

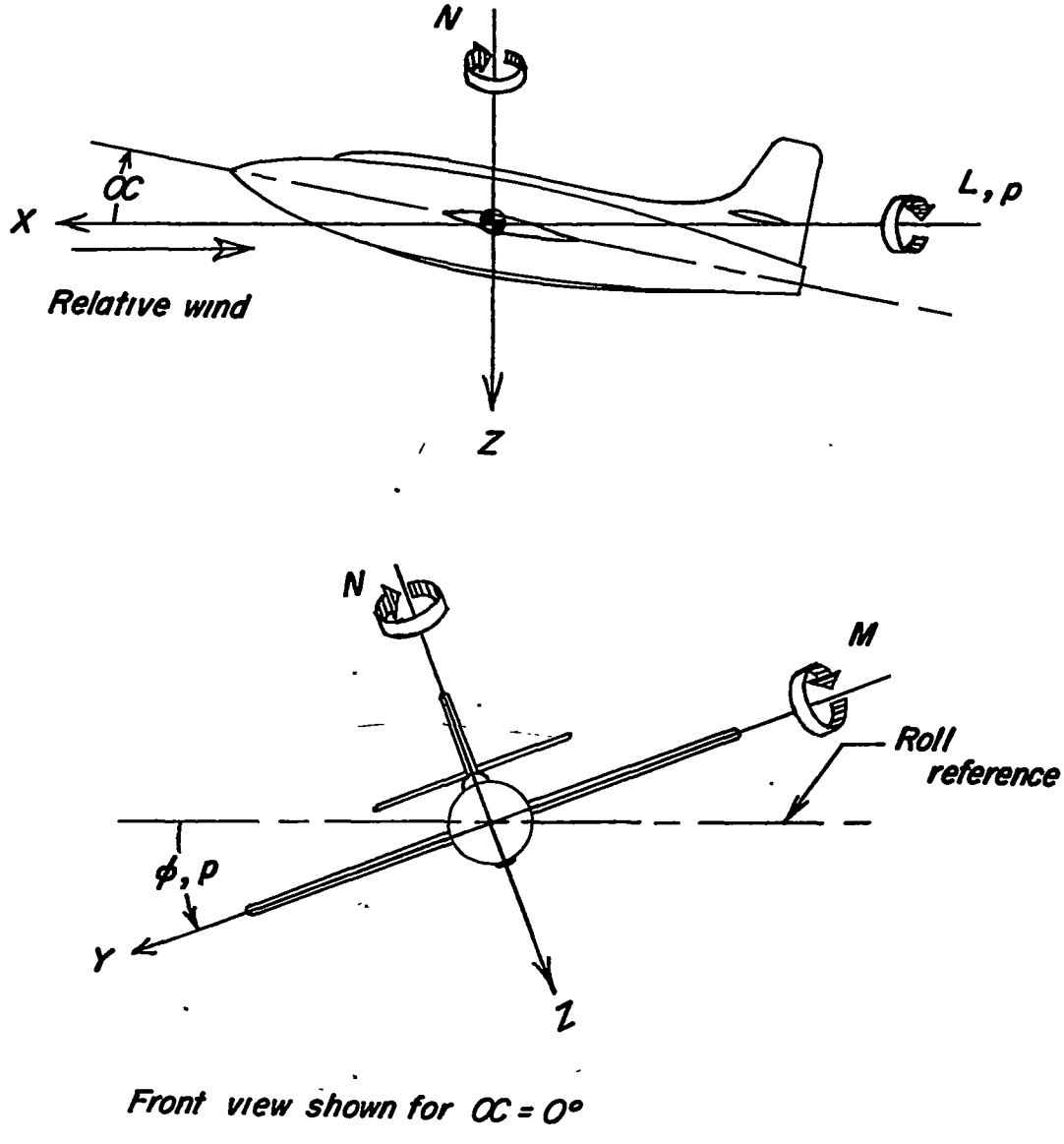

Figure 1.- System of stability axes. Arrows indicate positive forces, moments and angular displacements, and angular velocities.

$A_w = 6$

$\lambda_w = .5$

$\bar{c}_w = 0.479$ ft

$S_w = 1.3$ ft^2

$A_f = 2$

$S_f = .33$ ft^2

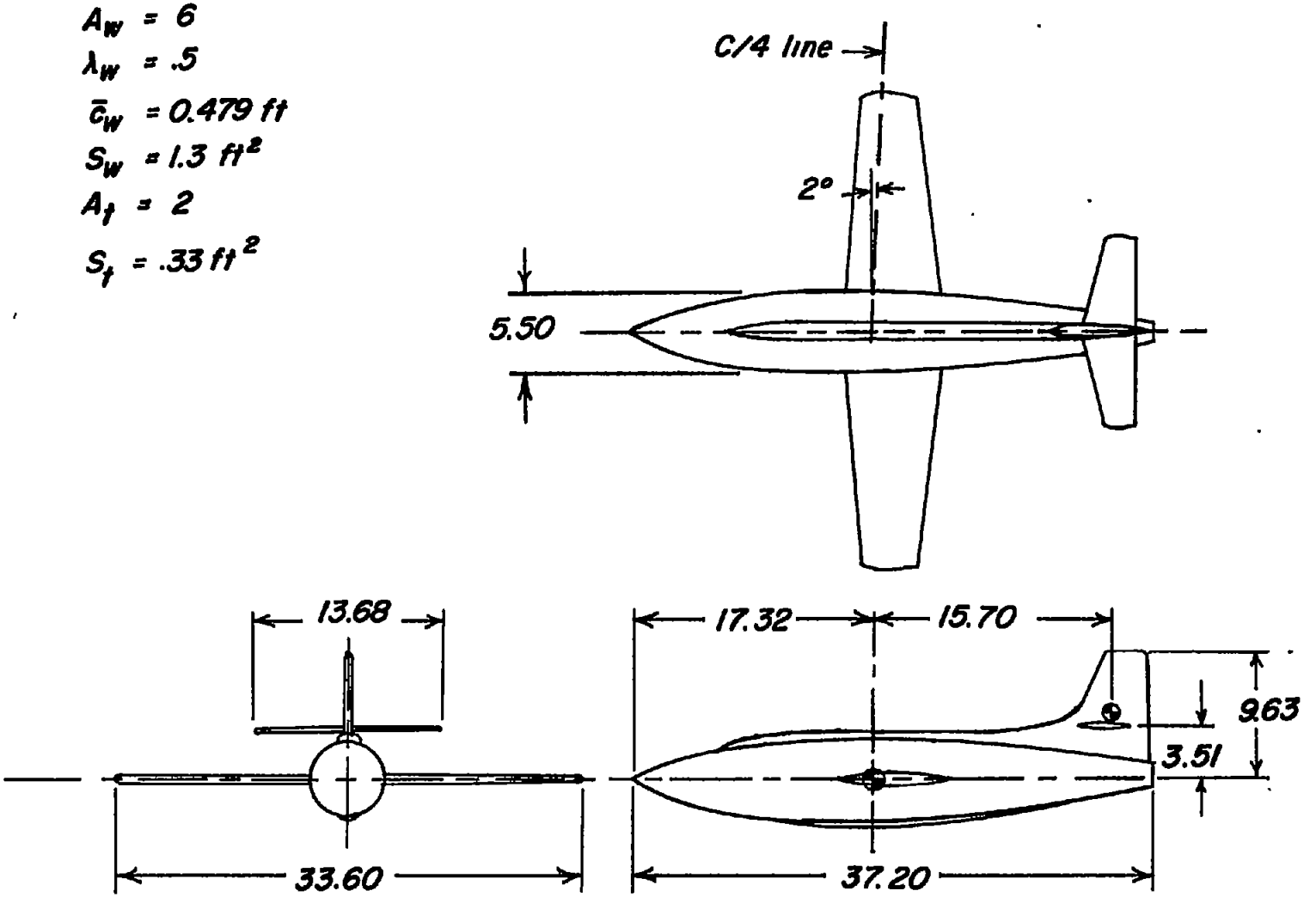

Figure 2.- Drawing of model tested. All dimensions are in inches.

L-83233

Figure 3.- Complete model on oscillation sting.

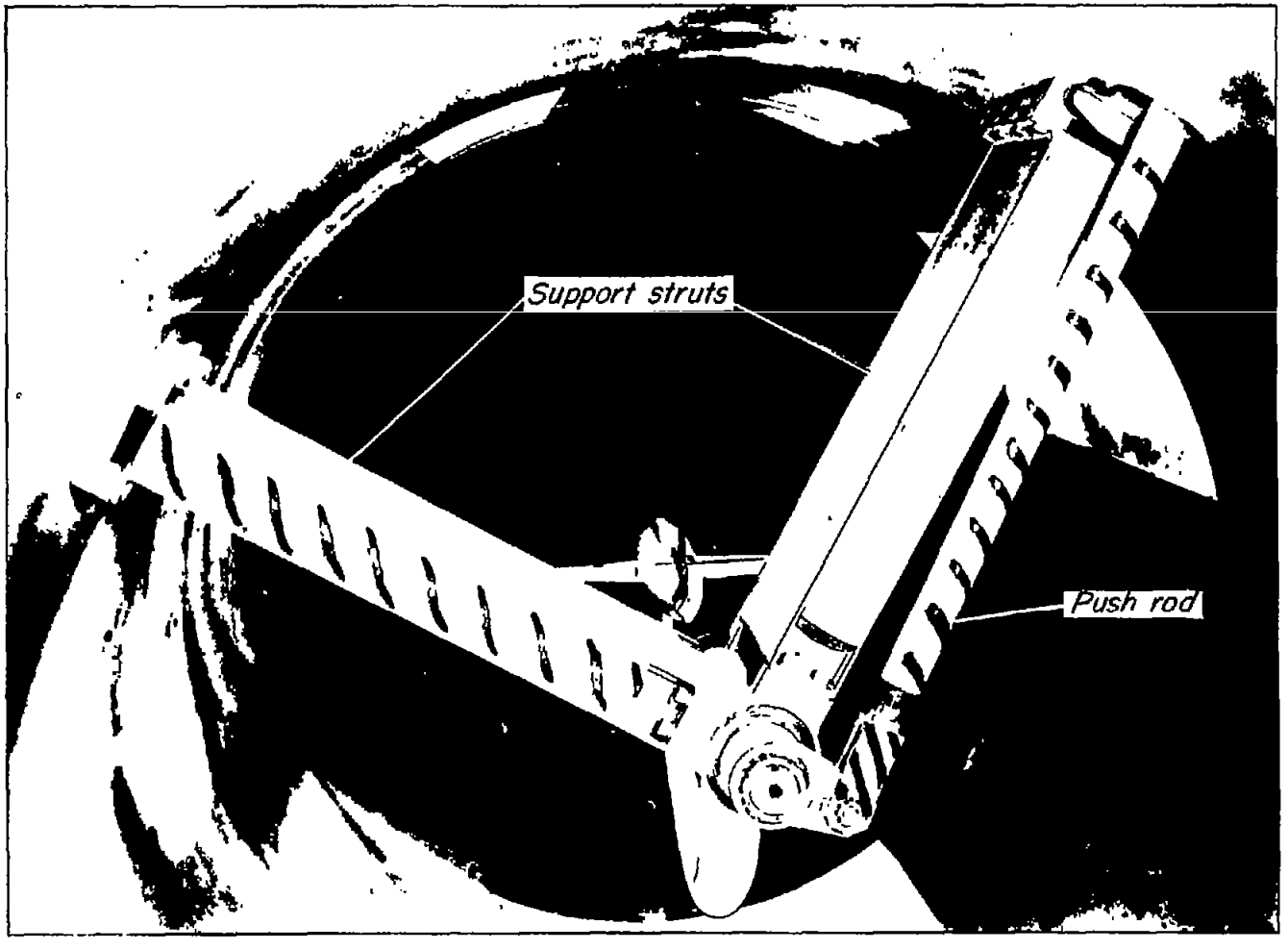

L-82969.1

(a) Inside tunnel.

Figure 4.- Oscillation apparatus.

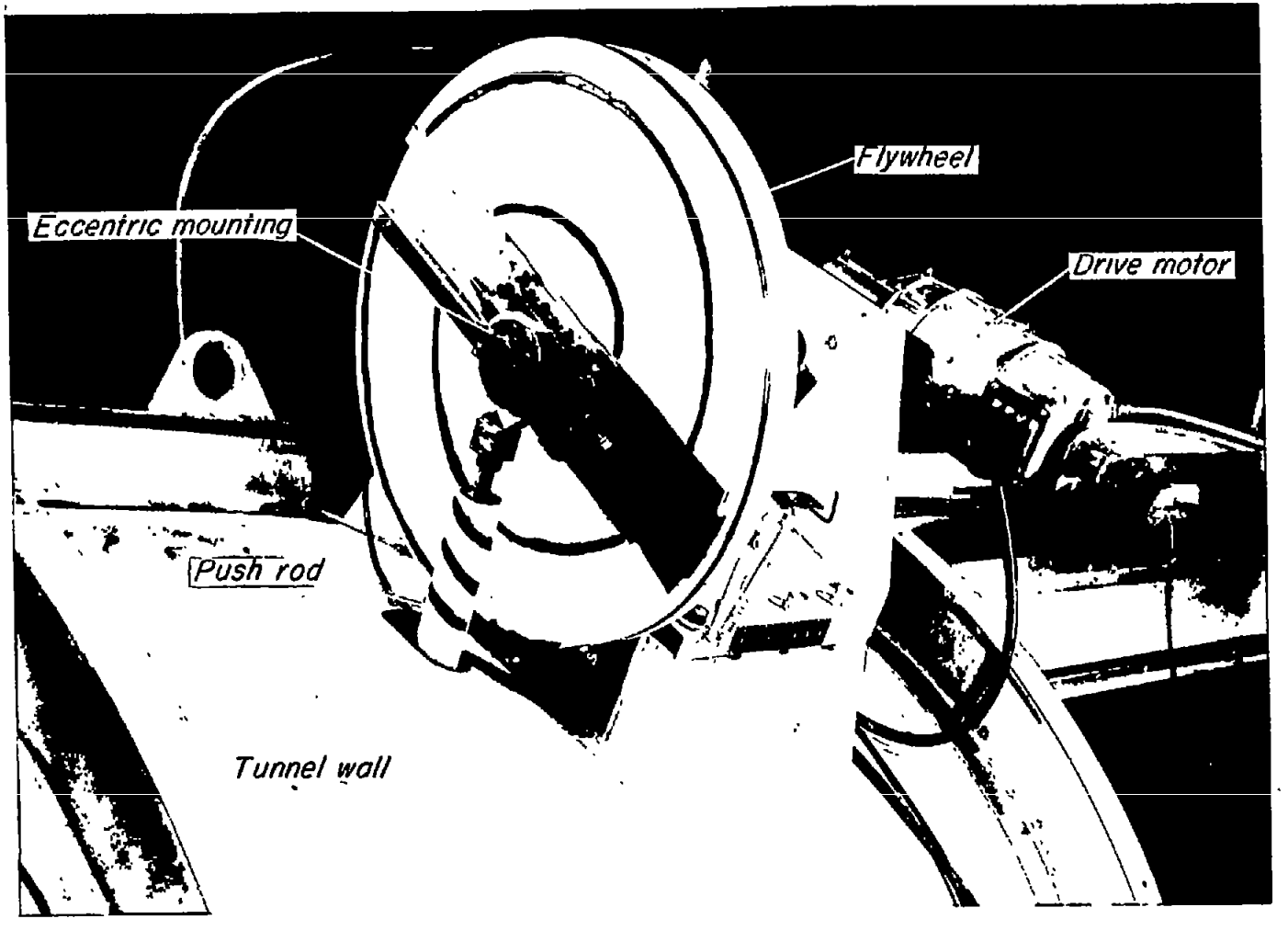

L-82970.1

(b) Outside tunnel.

Figure 4.- Concluded.

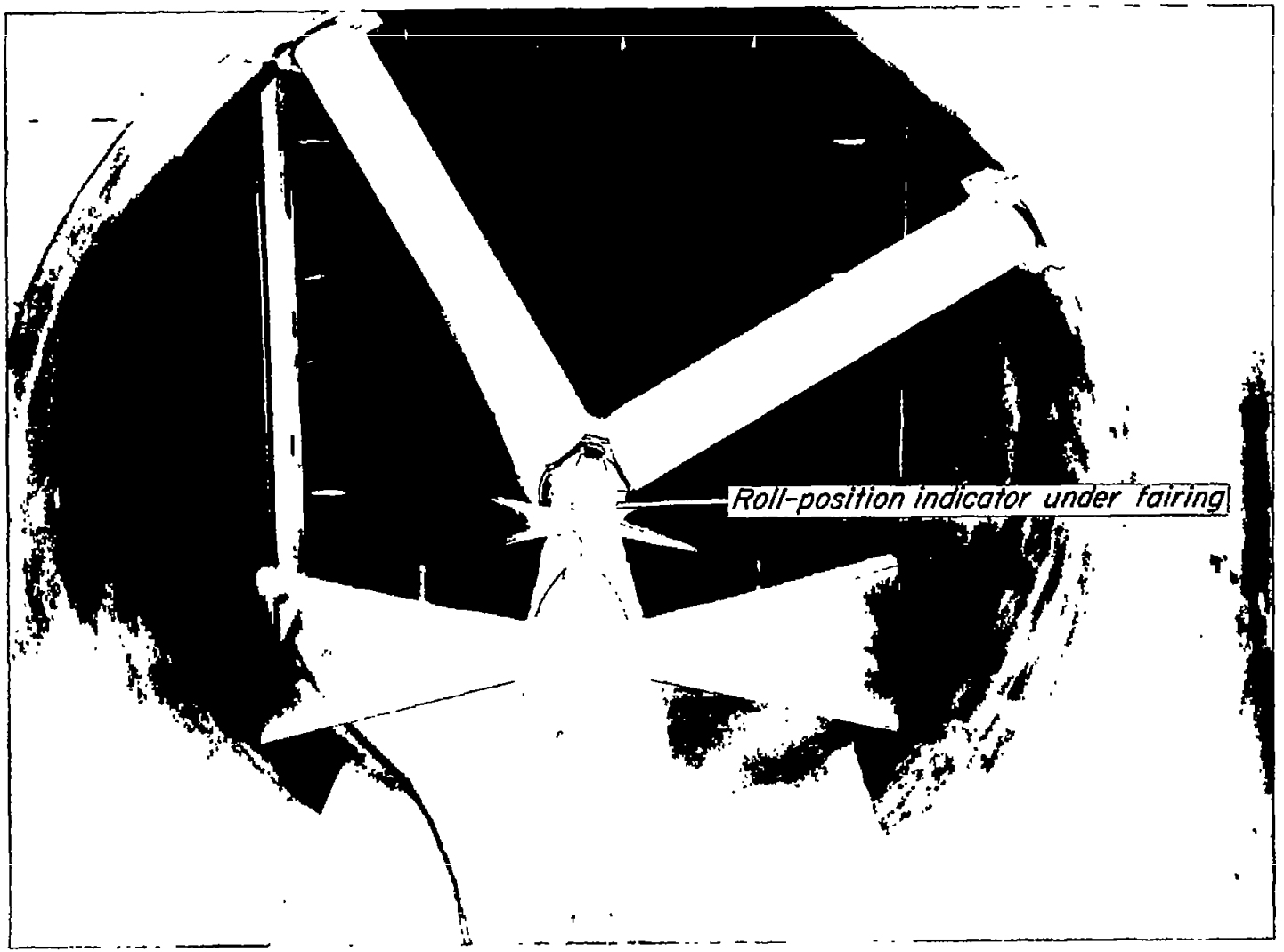

L-82973.1

Figure 5.- Typical motion of model during oscillation.

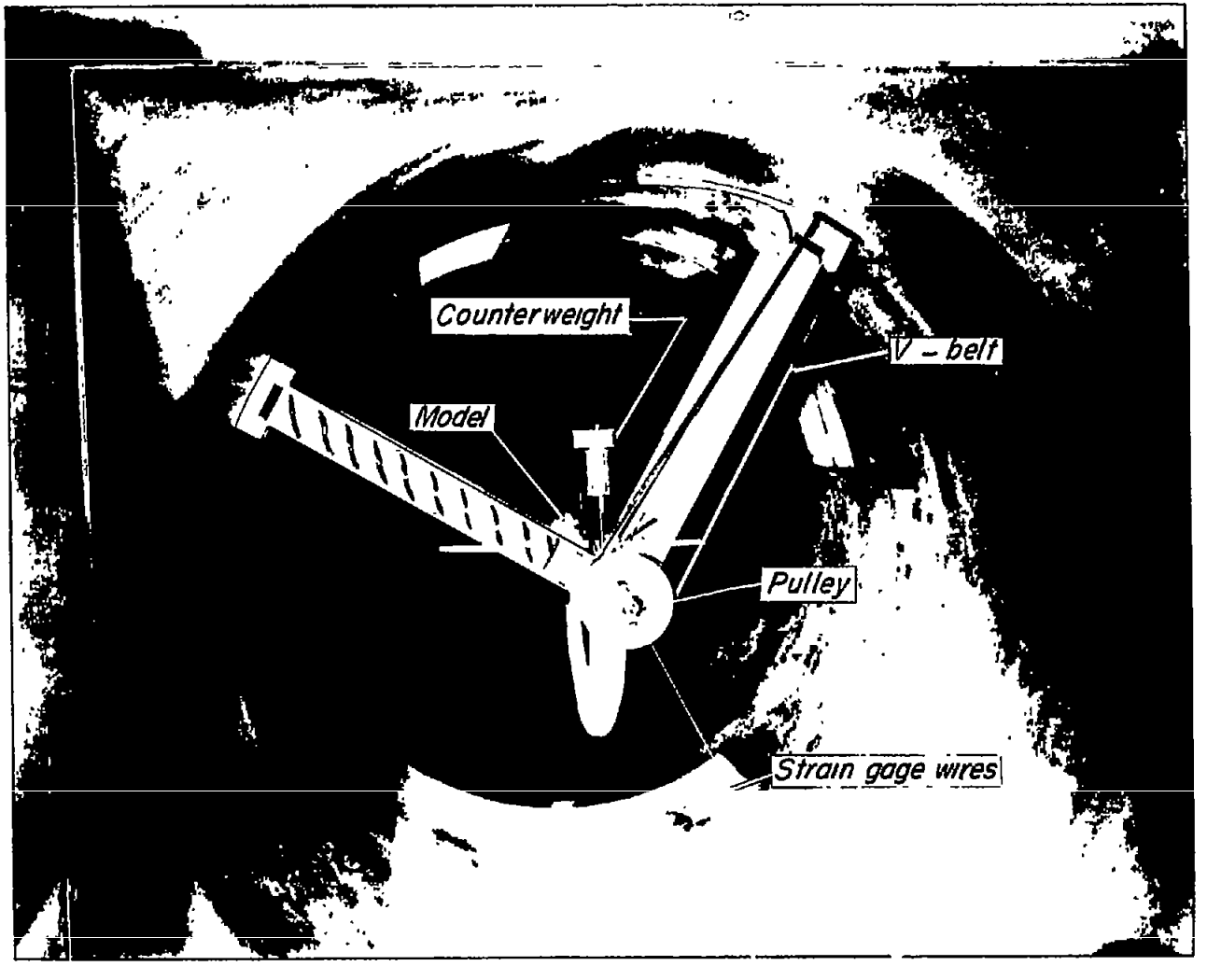

L-83236.1

Figure 6.- Modified apparatus for steady rolling of model.

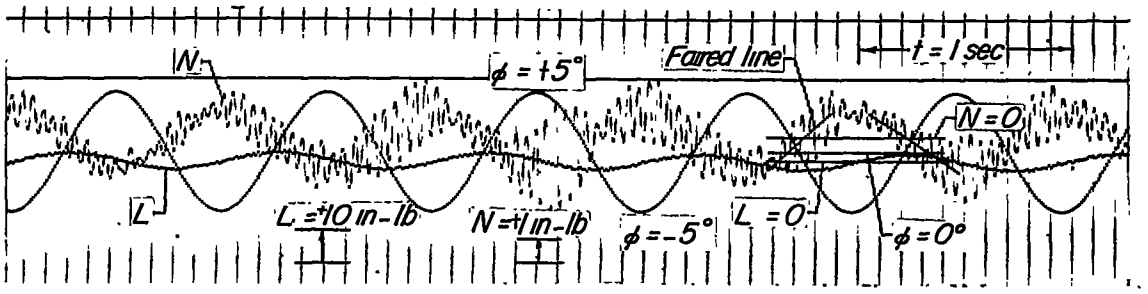

(a) $\alpha = 0^\circ$; $\phi_o = \pm 5^\circ$.

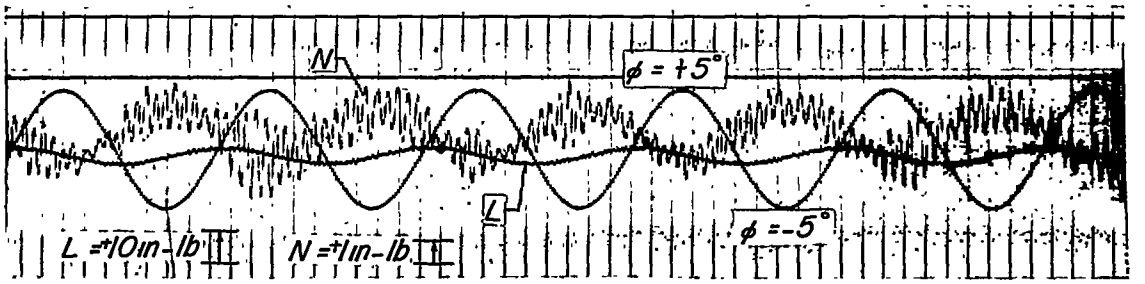

(b) $\alpha = 4^\circ$; $\phi_o = \pm 5^\circ$.

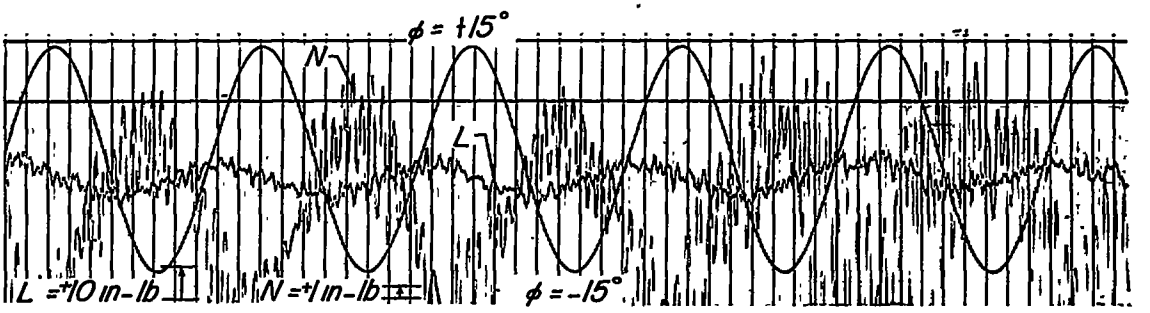

(c) $\alpha = 8^\circ$; $\phi_o = \pm 15^\circ$.

Figure 7.- Sample oscillograph records for three angles of attack. W + F + T; f = 1 cps.

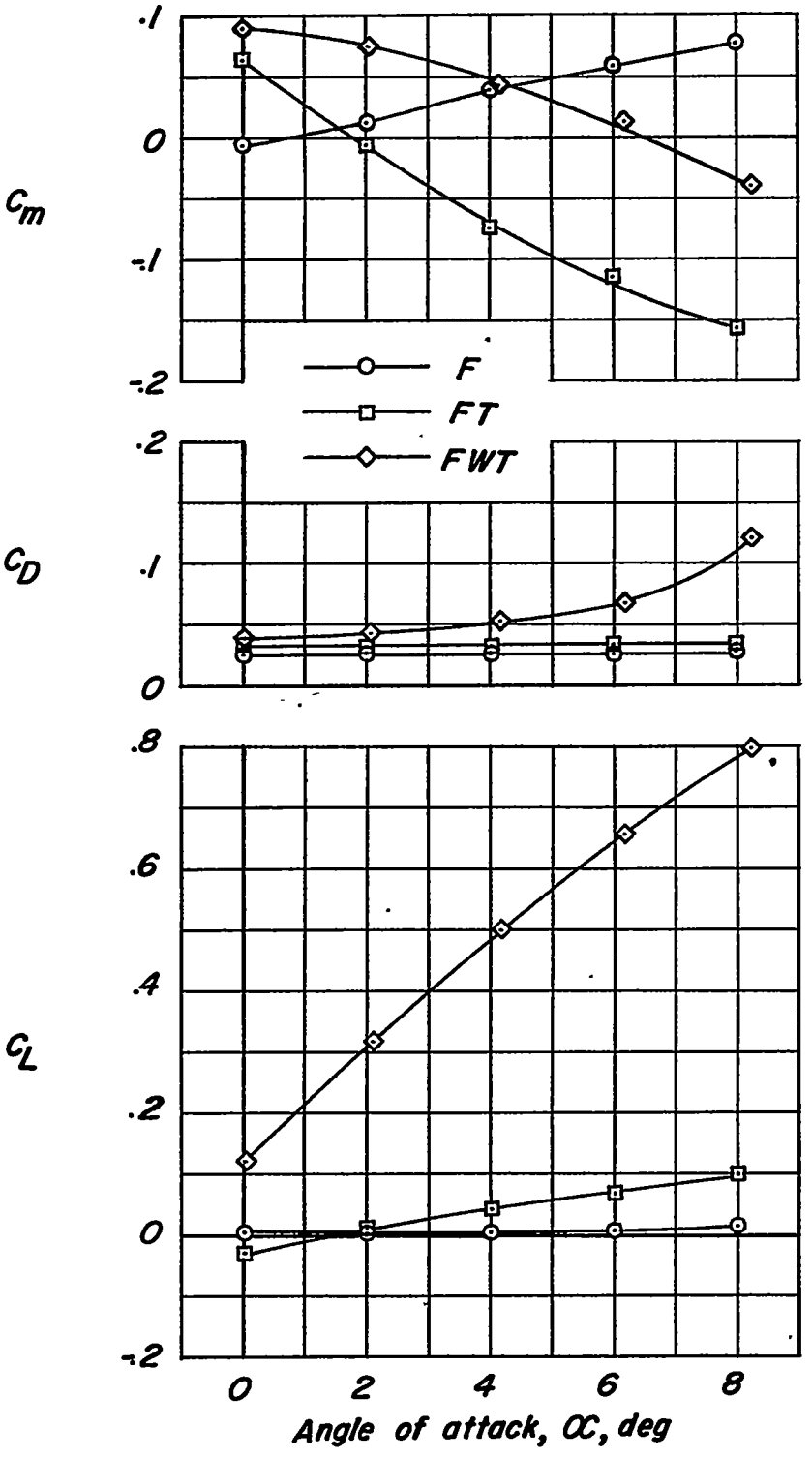

Figure 8.- Lift, drag, and pitching-moment characteristics of model tested. Data taken from reference 1.

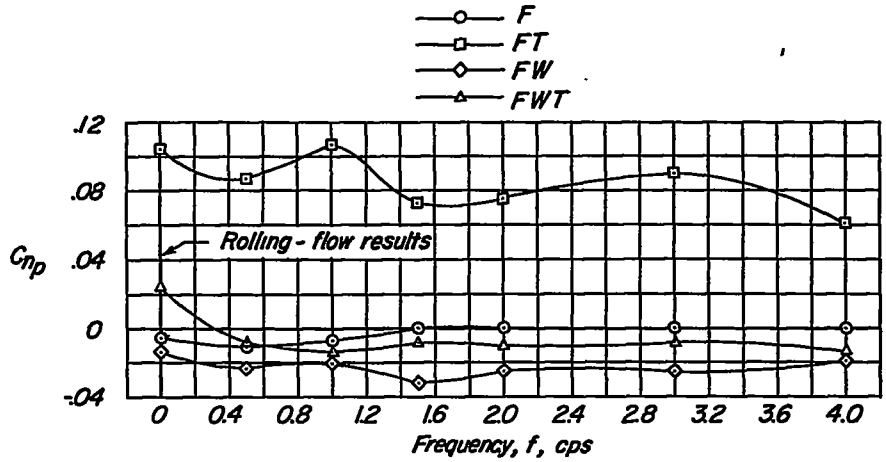

(a) Effect of frequency. $\alpha = 0^\circ$; $\phi_o = \pm 5^\circ$.

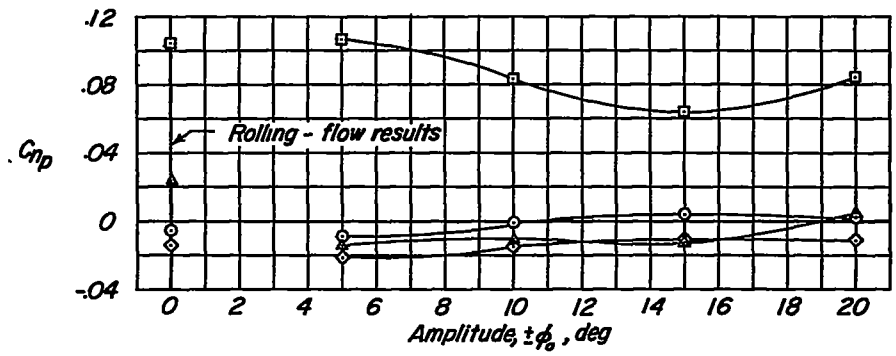

(b) Effect of amplitude. $\alpha = 0^\circ$; f = 1 cps.

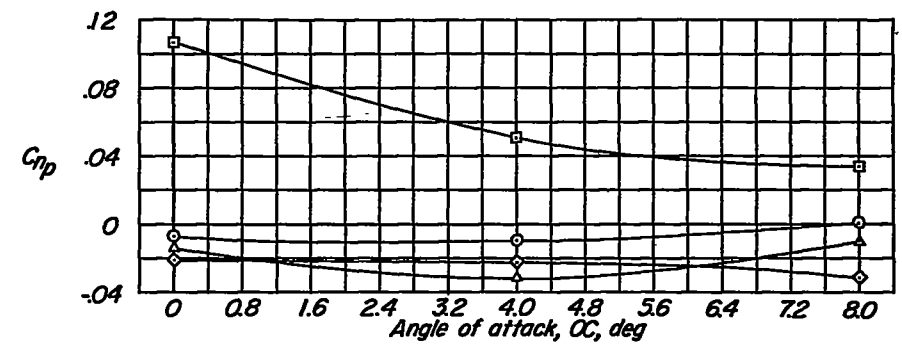

(c) Effect of angle of attack. $\phi_o = \pm 5^\circ$; f = 1 cps.

Figure 9.- The effects of frequency, amplitude, and angle of attack on the yawing moment due to rolling. Rolling-flow results are for model mounted on sting support.

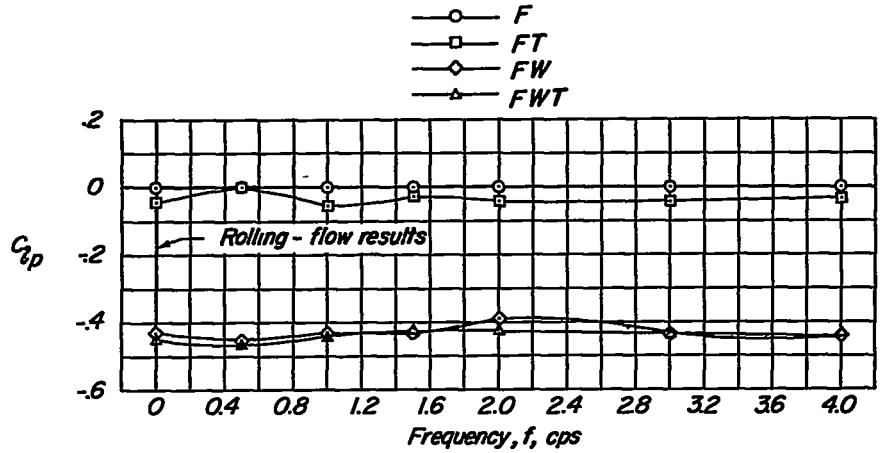

(a) Effect of frequency. $\alpha = 0^\circ$; $\phi_o = \pm 5^\circ$.

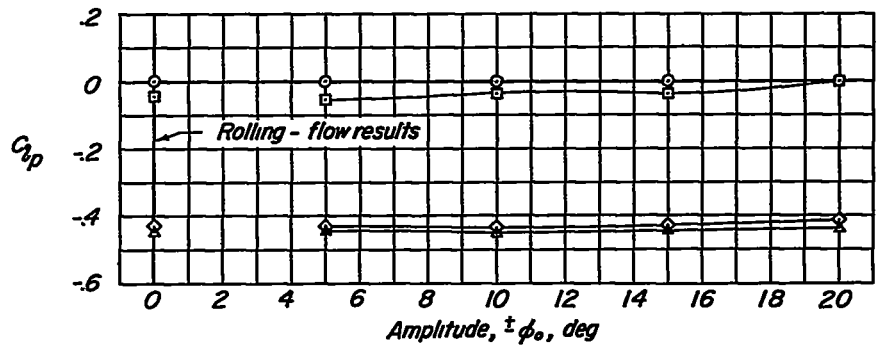

(b) Effect of amplitude. $\alpha = 0^\circ$; f = 1 cps.

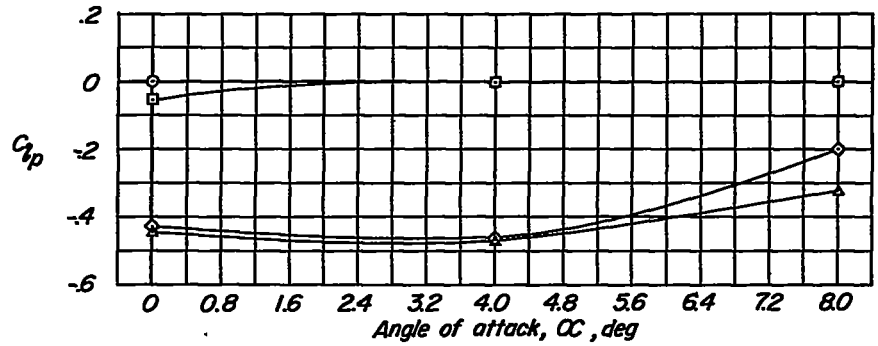

(c) Effect of angle of attack. $\phi_o = \pm 5^\circ$; f = 1 cps.

Figure 10.- The effects of frequency, amplitude, and angle of attack on the damping in roll. Rolling-flow results are for model mounted on sting support.

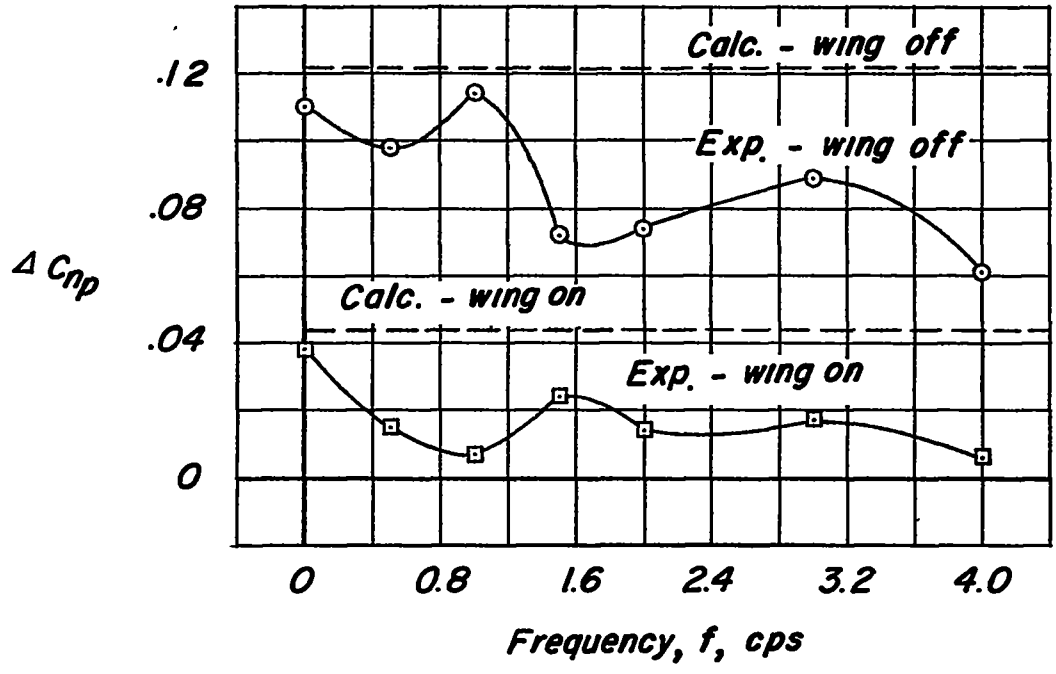

(a) Effect of frequency at $\phi = \pm 5^{\circ}$.

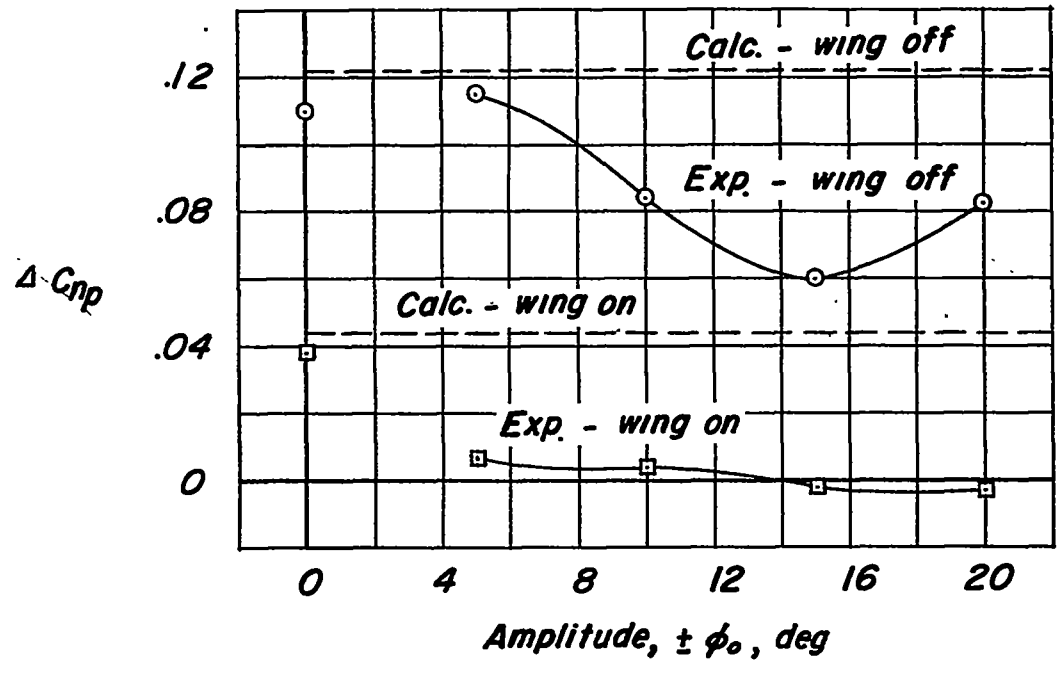

(b) Effect of amplitude at f = 1 cps.

Figure 11.- The effect of frequency and amplitude on the tail increment to the yawing moment due to rolling obtained at $\alpha = 0^{\circ}$.